

**[M]**acro-  
olecular  
Rapid Communications

Supporting Information

for *Macromol. Rapid Commun.*, DOI 10.1002/marc.202401082

Synthesis of Bithiazole-Based Poly(arylenevinylene)s via Co-Catalyzed Hydroarylation Polyaddition and Tuning of Their Optical Properties by *N*-Methylation and *N*-Oxidation

*Boya Li, Ryota Iwamori, Junpei Kuwabara, Takeshi Yasuda and Takaki Kanbara\**

## Supporting Information

### **Synthesis of Bithiazole-Based Poly(arylenevinylene)s via Co-Catalyzed Hydroarylation Polyaddition and Tuning of their Optical Properties by *N*-Methylation and *N*-Oxidation**

*Boya Li*<sup>a</sup>, *Ryota Iwamori*<sup>a</sup>, *Junpei Kuwabara*<sup>a,b</sup>, *Takeshi Yasuda*<sup>c</sup> and *Takaki Kanbara*<sup>a\*</sup>

<sup>a</sup> Institute of Pure and Applied Sciences, University of Tsukuba, 1-1-1 Tennodai, Tsukuba, Ibaraki, 305-8573, Japan.

<sup>b</sup> Tsukuba Research Center for Energy Materials Science (TREMS), Institute of Pure and Applied Sciences, University of Tsukuba, 1-1-1 Tennodai, Tsukuba, Ibaraki 305-8573, Japan.

<sup>c</sup> Research Center for Macromolecules and Biomaterials, National Institute for Materials Science (NIMS), 1-2-1 Sengen, Tsukuba, Ibaraki 305-0047, Japan.

Corresponding Author

Takaki Kanbara\* (E-mail: [kanbara@ims.tsukuba.ac.jp](mailto:kanbara@ims.tsukuba.ac.jp))

### **Experimental section**

#### **Materials**

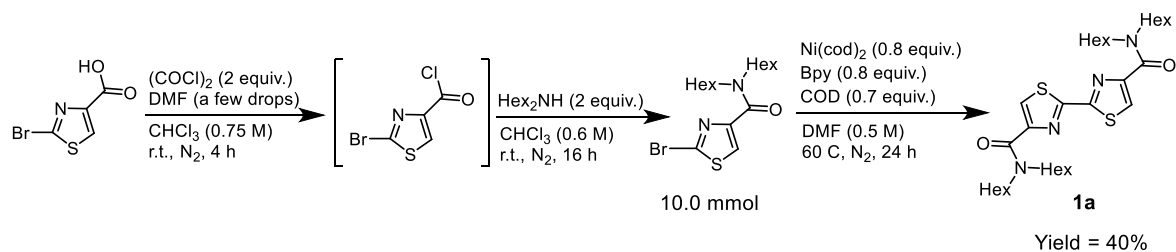
All reagents from commercial sources were used without further purification unless otherwise noted. Anhydrous solvents were purchased from Kanto Chemical. 4-Ethynyltoluene (**2a**) was purchased from Tokyo Chemical Industry. Neodecanoic acid (NDA) was purchased from Wako Pure Chemical Industries. The other reagents were also purchased from Tokyo Chemical Industry. The synthesis of *N,N,N',N'*-tetrahexyl-(2,2'-bithiazole)-4,4'-dicarboxamide (**1a**) is described in Supporting Information. 2,7-Diethynyl-9,9-bis(2-ethylhexyl)fluorene (**4a**), 2,7-bis(4-ethynylphenyl)-9,9-di(*n*-octyl)fluorene (**4b**), and [Cp\*Co(CH<sub>3</sub>CN)<sub>3</sub>](SbF<sub>6</sub>)<sub>2</sub> were synthesized by the same methods as our previous report.<sup>[1]</sup>

#### **General methods**

NMR spectra were recorded on Bruker AVANCE-400 and AVANCE-600 NMR spectrometers. <sup>1</sup>H NMR spectra were measured with CHCl<sub>3</sub> (7.26 ppm for <sup>1</sup>H NMR), C<sub>2</sub>HDCl<sub>4</sub> (6.00 ppm for <sup>1</sup>H NMR), and acetone-*d*<sub>6</sub> (2.05 ppm for <sup>1</sup>H NMR) as an internal reference. GPC

measurements were carried out on a SHIMADZU prominence GPC system equipped with polystyrene gel columns, using THF as an eluent after calibration with polystyrene standards at 40 °C. High-resolution mass spectroscopy (HRMS) was carried out with an APCI-Direct Probe of Bruker micrOTOF II. Elemental analyses were carried out with Yanaco CHN coder MT-6 or MT-5. FT-IR spectra were recorded on a JASCO FT/IR-4600. UV-vis absorption spectra in solution states were recorded on a Hitachi U-3900H. PL spectra in solution states were recorded on a Hitachi F-2700 fluorescence spectrophotometers. PLQYs in solution were measured using a Hamamatsu Photonics C9920-02. UV-vis absorption spectra and PL spectra for the spin-coated films were recorded on a Hitachi U-3010 and JASCO FP-6500 spectrophotometer, respectively. PLQYs of the spin-coated films were measured using a JASCO FP-6500 spectrophotometer with an integrating sphere. The HOMO energy levels were estimated by ultraviolet photoelectron spectroscopy (UPS), and the LUMO energy levels were estimated by low-energy inverse photoelectron spectroscopy (LEIPS), using PHI VersaProbe 4 of Ulvac PHI. All of the manipulations for the reactions were performed under a nitrogen atmosphere using Schlenk techniques.

### Synthesis of **1a** (Figures S9 and Figures S10)



2-Bromo-*N,N*-dihexylthiazole-4-carboxamide was prepared referring to procedures reported in the literature.<sup>[2]</sup> A mixture of 2-bromo-*N,N*-dihexylthiazole-4-carboxamide (3.75 g, 10.0 mmol), 2,2'-bipyridine (1.25 g, 8.0 mmol), Ni(cod)<sub>2</sub> (2.20 g, 8.0 mmol), cycloocta-1,5-diene (859 μL, 7.0 mmol) was stirred in *N,N*-dimethylformamide (20 mL) at 60 °C for 24 h under nitrogen atmosphere.<sup>[3,4]</sup> Then, the reaction mixture was cooled to room temperature. The organic compound was extracted with toluene and washed with distilled water and brine. The organic layer was dried over sodium sulfate and filtered through a Celite plug. The product was isolated by silica gel column chromatography using hexane : ethyl acetate (9:1 → 4:1) as an eluent. *N,N,N',N'*-tetrahexyl-(2,2'-bithiazole)-4,4'-dicarboxamide (**1a**) was obtained as a pale yellow solid (1.2 g, 40% yield). <sup>1</sup>H NMR (400 MHz, CDCl<sub>3</sub>): δ = 8.05 (s, 2H), 3.41–3.71 (m,

8H), 1.70 (br m, 8H), 1.31 (br m, 24H), 0.88 (br m, 12H). HRMS (APCI):  $m/z$  calculated for  $C_{32}H_{55}N_4O_2S_2^+$   $[M+H]^+$ : 591.3766, found: 591.3767

### General procedure of small molecular model reactions

To a stirred solution of **1a** (59.1 mg, 0.10 mmol) in anhydrous DCE (2.0 mL) was added 4-ethynyltoluene (**2a**, 26.6  $\mu$ L, 0.21 mmol) and 1,3,5-trimethoxybenzene (11.1 mg, 0.066 mmol). Then,  $[Cp^*Co(CH_3CN)_3](SbF_6)_2$  (1.58 mg, 0.0020 mmol) and NDA (5.68  $\mu$ L, 0.030 mmol) were added. The reaction mixture was stirred for 24 h at 30 °C under a nitrogen atmosphere. A portion of the reaction mixture was sampled at 0, 1 and 24 h. The NMR yield was calculated from the integral value of the signal for the product based on the internal standard (1,3,5-trimethoxybenzene). The isolation of the product is described below.

### Synthesis of **3aa**

The reaction mixture was diluted with  $CHCl_3$  (50 mL) and poured into  $NH_3$  solution (28% in water, 50 mL). The organic layer was washed with  $NH_3$  solution and distilled water (100 mL x 2). The organic layer was dried over sodium sulfate and filtered through a Celite plug. The product was isolated by silica gel column chromatography using hexane : ethyl acetate (9:1) as an eluent. **3aa** was obtained as a red solid in 81% yield (70.8 mg).  $^1H$  NMR (600 MHz,  $CDCl_3$ , r.t.):  $\delta$  = 7.47 (d,  $J$  = 15.3, 2H), 7.38 (d,  $J$  = 8.0, 4H), 7.16 (d,  $J$  = 7.6, 4H), 6.98 (d,  $J$  = 15.8, 2H), 3.24–3.61 (m, 8H), 2.36 (s, 2H), 1.71 (br m, 8H), 1.27 (br m, 24H), 0.88 (br m, 12H).

### Synthesis of **Pab**

To a stirred solution of **1a** (59.1 mg, 0.10 mmol) and **4b** (59.1 mg, 0.10 mmol) in anhydrous DCE (2.0 mL) were added  $[Cp^*Co(CH_3CN)_3](SbF_6)_2$  (1.58 mg, 0.0020 mmol) and NDA (5.68  $\mu$ L, 0.030 mmol). The reaction mixture was stirred for 10 min at 70 °C under a nitrogen atmosphere. Then, the reaction mixture was diluted with  $CHCl_3$  (50 mL) and poured into  $NH_3$  solution (28% in water, 50 mL). The organic layer was washed with  $NH_3$  solution and distilled water (100 mL x 2). The organic layer was dried over sodium sulfate and filtered through a Celite plug. The solution of  $CHCl_3$  was concentrated and reprecipitated into methanol. The precipitate was collected by filtration and dried under vacuum. A polymeric product (**Pab**) was obtained as a yellow solid in 96% yield (113 mg,  $M_n$  = 68,000,  $M_w/M_n$  = 3.6).  $^1H$  NMR (600 MHz,  $C_2D_2Cl_4$ , 373 K):  $\delta$  = 7.83 (s, 2H), 7.74 (s, 4H), 7.67 (m, 8H), 7.57 (d,  $J$  = 1.6, 2H), 7.17 (d,  $J$  = 15.7, 2H), 3.60 (br s, 8H), 2.12 (br s, 4H), 1.66–2.01 (br s, 8H), 1.12–1.46 (br m, 44H),

0.66–1.12 (br m, 22H). Anal. calcd. for  $C_{77}H_{104}N_4O_2S_2$ : C 78.26, H 8.87, N 4.74; found: C 78.35, H 8.96, N 4.82.

### Synthesis of Paa-M-11

A solution of **Paa** (20.6 mg, 0.020 mmol based on the repeating unit) and MeOTf (7.92  $\mu$ L, 0.070 mmol) in anhydrous  $CHCl_3$  (2.0 mL) was stirred for 7 days at 50 °C under a nitrogen atmosphere. During the reaction, the color of the solution gradually changed from orange to red. The reaction product was concentrated and reprecipitated into hexane. The precipitate was washed with water and dried under vacuum. An *N*-methylated product (**Paa-M-11**) was obtained as a purple solid in 69% yield. (calculated based on the *N*-methylation ratio, 14.7 mg)  $^1H$  NMR (600 MHz, Acetone- $d_6$ , r.t.):  $\delta$  = 7.23–8.06 (m, 10H, aromatic C–H bonds), 4.46–4.64 (s, 0.66 H, *N*- $CH_3$ ), 3.23–3.85 (m, 8H,  $\alpha$ -methylene protons of alkyl amides). 2.13–2.37 (br s, 8H), 1.62–1.90 (m, 8H), 1.28 (m, 24H), 0.39–1.09 (m, 42H). The *N*-methylation ratio = 11%

### Synthesis of Paa-M-27

A solution of **Paa** (20.6 mg, 0.020 mmol based on the repeating unit) and MeOTf (31.7  $\mu$ L, 0.28 mmol) in anhydrous  $CHCl_3$  (2.0 mL) was stirred for 7 days at 50 °C under a nitrogen atmosphere. During the reaction, the color of the solution gradually changed from orange to red. The reaction product was concentrated and reprecipitated into hexane. The precipitate was washed with water and dried under vacuum. An *N*-methylated product (**Paa-M-27**) was obtained as a purple solid in 62% yield. (calculated based on the *N*-methylation ratio, 13.9 mg)  $^1H$  NMR (600 MHz, Acetone- $d_6$ , r.t.):  $\delta$  = 7.23–8.15 (m, 10H, aromatic C–H bonds), 4.55 (s, 1.64 H, *N*- $CH_3$ ), 3.21–3.86 (m, 8H,  $\alpha$ -methylene protons of alkyl amides). 2.11–2.37 (br s, 8H), 1.59–1.91 (m, 8H), 1.08–1.59 (m, 24H), 0.31–1.08 (m, 42H). The *N*-methylation ratio = 27%

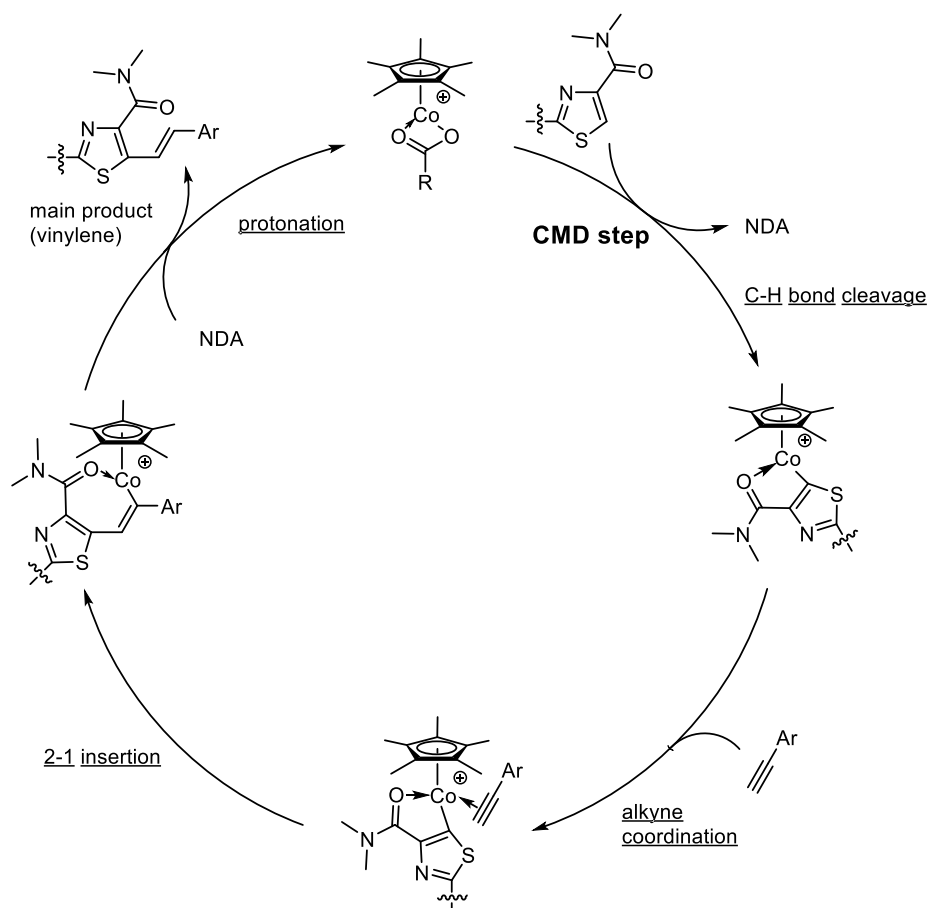
### Synthesis of Paa-M-50

A solution of **Paa** (20.6 mg, 0.020 mmol based on the repeating unit) and MeOTf (15.8  $\mu$ L, 0.14 mmol) in anhydrous  $CHCl_3$  (2.0 mL) was stirred for 7 d at 70 °C under a nitrogen atmosphere. During the reaction, the color of the solution gradually changed from orange to red. The reaction product was concentrated and reprecipitated into hexane. The precipitate was washed with water and dried under vacuum. An *N*-methylated product (**Paa-M-50**) was obtained as a purple solid in 66% yield. (calculated based on the *N*-methylation ratio, 15.7 mg)

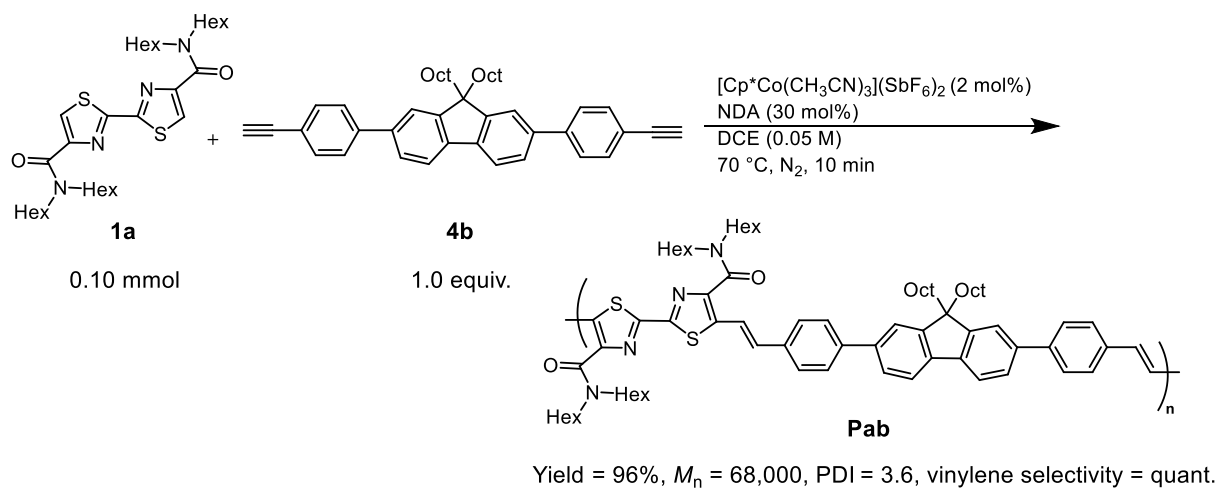
$^1\text{H}$  NMR (600 MHz, Acetone- $d_6$ , r.t.):  $\delta$  = 7.25–8.19 (m, 10H, aromatic C–H bonds), 4.54 (s, 2.99 H, *N*-CH<sub>3</sub>), 3.22–3.95 (m, 8H,  $\alpha$ -methylene protons of alkyl amides). 2.15 (br s, 8H), 1.59–2.01 (m, 8H), 1.08–1.59 (m, 24H), 0.85 (m, 42H). The *N*-methylation ratio = 50%

### **Fabrication and Characterization of OLED.**

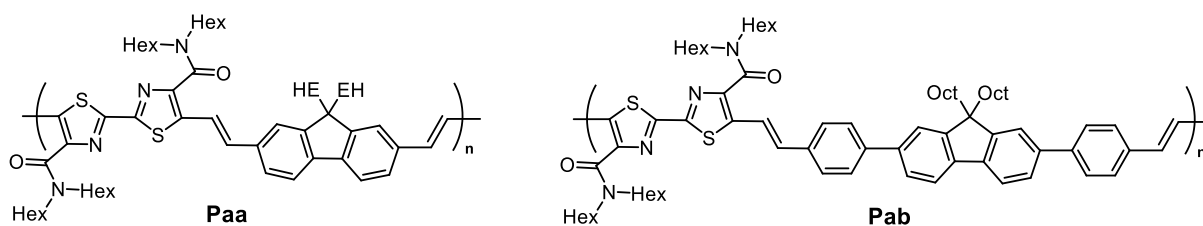
OLED was fabricated in the following configuration: ITO/PEDOT:PSS/light-emitting **Paa-O** (2.9 wt%)-doped PVK/electron transporting (hole blocking) diphenyl[9,9'-spirobifluoren-2-yl]phosphine oxide (SPPO1) layer/LiF/Al. The patterned indium tin oxide (ITO) glass (conductivity: 10  $\Omega$ /square) was treated in an ultraviolet-ozone chamber. A thin layer (40 nm) of PEDOT:PSS was spin-coated onto the ITO at 3000 rpm and air-dried at 110 °C for 10 min on a hot plate. The substrate was then transferred to an N<sub>2</sub>-filled glovebox, where it was redried at 110 °C for 10 min on a hot plate. A 1.0 mL of THF solution of **Paa-O** (0.12 mg) and PVK (4.0 mg) was subsequently spin-coated onto the PEDOT:PSS surface to form the light-emitting and hole-transporting layer (44 nm). SPPO1 (40 nm), LiF (1 nm), and Al (100 nm) were then deposited onto the active layer with conventional thermal evaporation at a chamber pressure lower than 5 x 10<sup>-4</sup> Pa, which provided the devices with an active area of 2 x 2 mm<sup>2</sup>. Current–voltage characteristics and luminance of the OLED were simultaneously measured using an ADCMT 6245 DC voltage current source/monitor (ADC CORPORATION) and an LS-100 luminance meter (KONICA MINOLTA JAPAN, INC.), respectively. The EL spectra and the coordinates of the CIE chromaticity were measured using an array spectrometer (MCPD-9800-311C, Otsuka Electronics Co, Ltd.).



**Scheme S1. Proposed catalytic cycle of hydroarylation reaction of 1a**

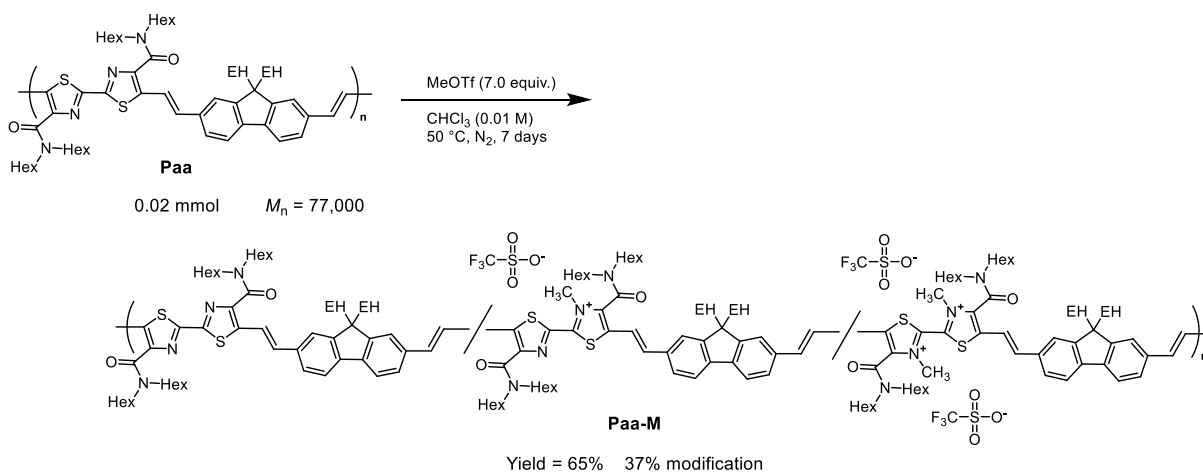


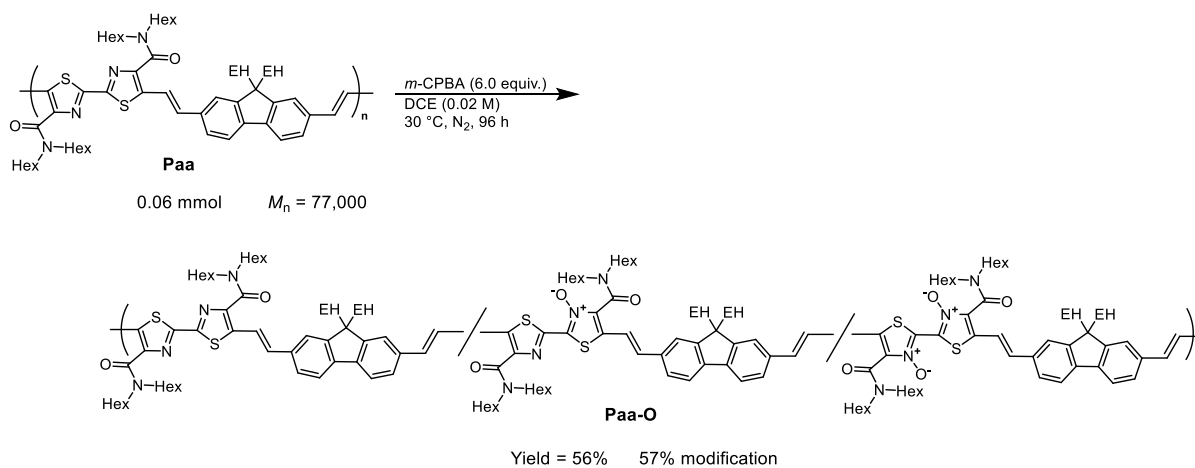
**Scheme S2. Hydroarylation polyaddition of 1a with 4b**

**Table S1. Hydroarylation polyaddition of 1a with 4a or 4b <sup>a</sup>**

Entry	PAV	Temp. /°C	Time	Yield <sup>b</sup> /%	$M_n$ <sup>c</sup>	$M_w/M_n$ <sup>c</sup>
1	<b>Paa</b>	30	1 h	82	5,400	1.5
2	<b>Paa</b>	30	4 h	91	40,000	2.8
3	<b>Paa</b>	70	4 h	92	77,000	3.0
4	<b>Pab</b>	30	4 h	93	34,000	3.1
5	<b>Pab</b>	70	10 min	96	68,000	3.6

<sup>a</sup> Equivalent C–H monomer (0.10 mmol), diyne monomer (0.10 mmol),  $[Cp^*Co(CH_3CN)_3](SbF_6)_2$  (0.0020 mmol, 1.58 mg), and NDA (0.030 mmol, 5.68  $\mu$ L) in DCE (0.05 M) at the prescribed temperature for the prescribed reaction time. <sup>b</sup> The products were obtained by reprecipitation from  $CHCl_3$ - $CH_3OH$ . <sup>c</sup> Estimated by GPC calibrated on polystyrene standards using THF as an eluent at 40 °C.

**Scheme S3. N-methylation reaction of Paa**



**Scheme S4. N-oxidation reaction of Paa**

**$^1\text{H}$  NMR and MS spectra**

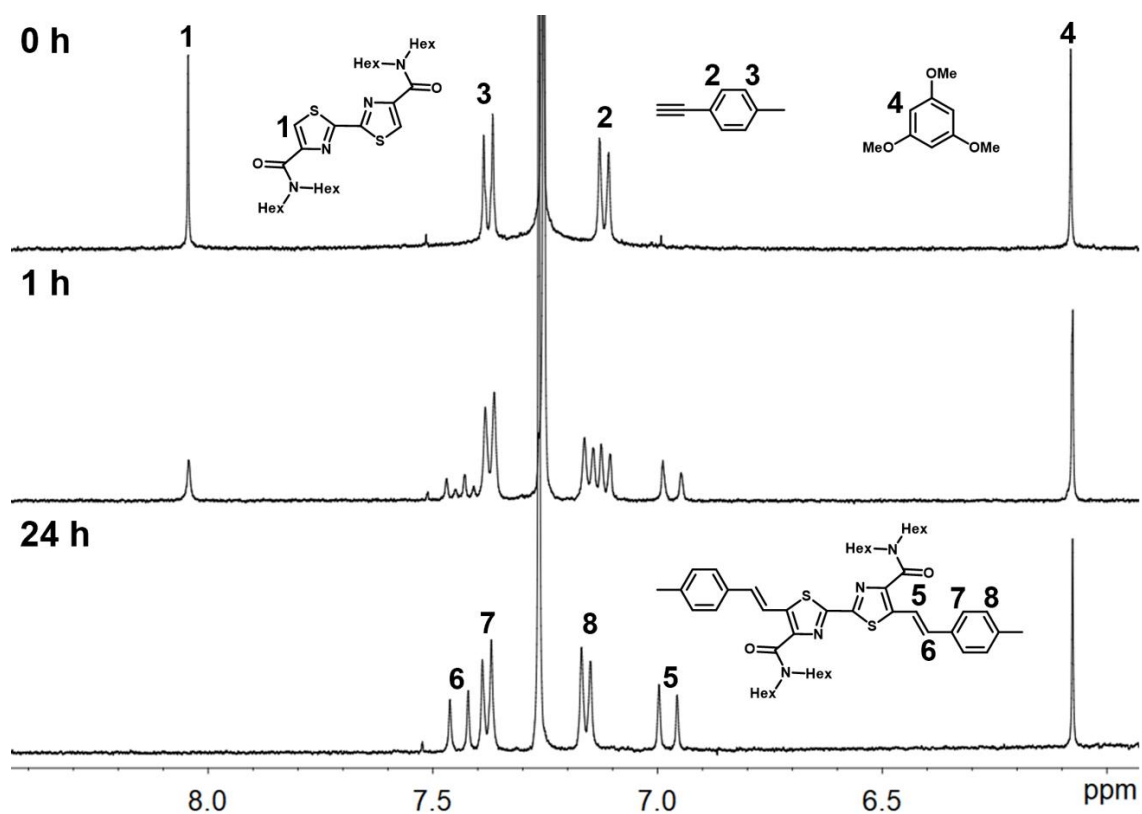


**Figure S1.  $^1\text{H}$  NMR spectra of the model reaction of 1a with 4-ethynyltoluene (400 MHz,  $\text{CDCl}_3$ , r.t.).**

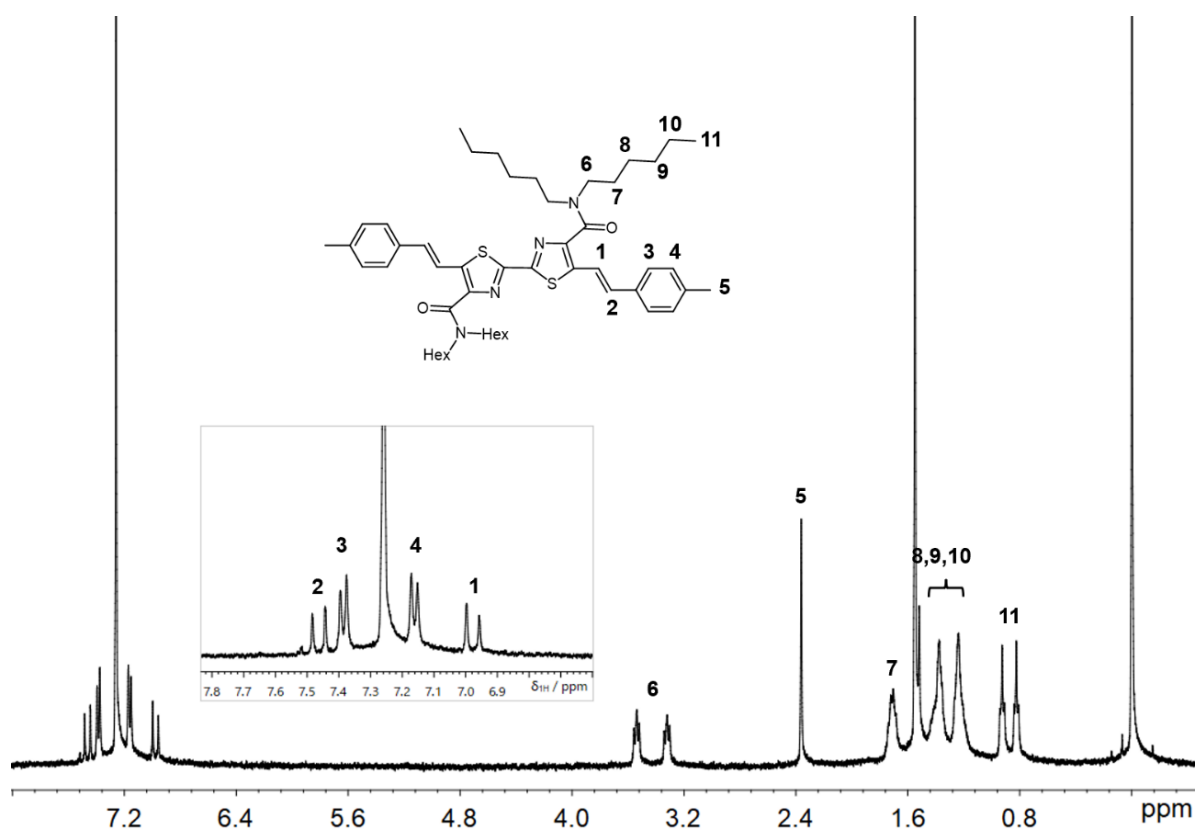


Figure S2.  $^1\text{H}$  NMR spectrum of 3aa (400 MHz,  $\text{CDCl}_3$ , r.t.).

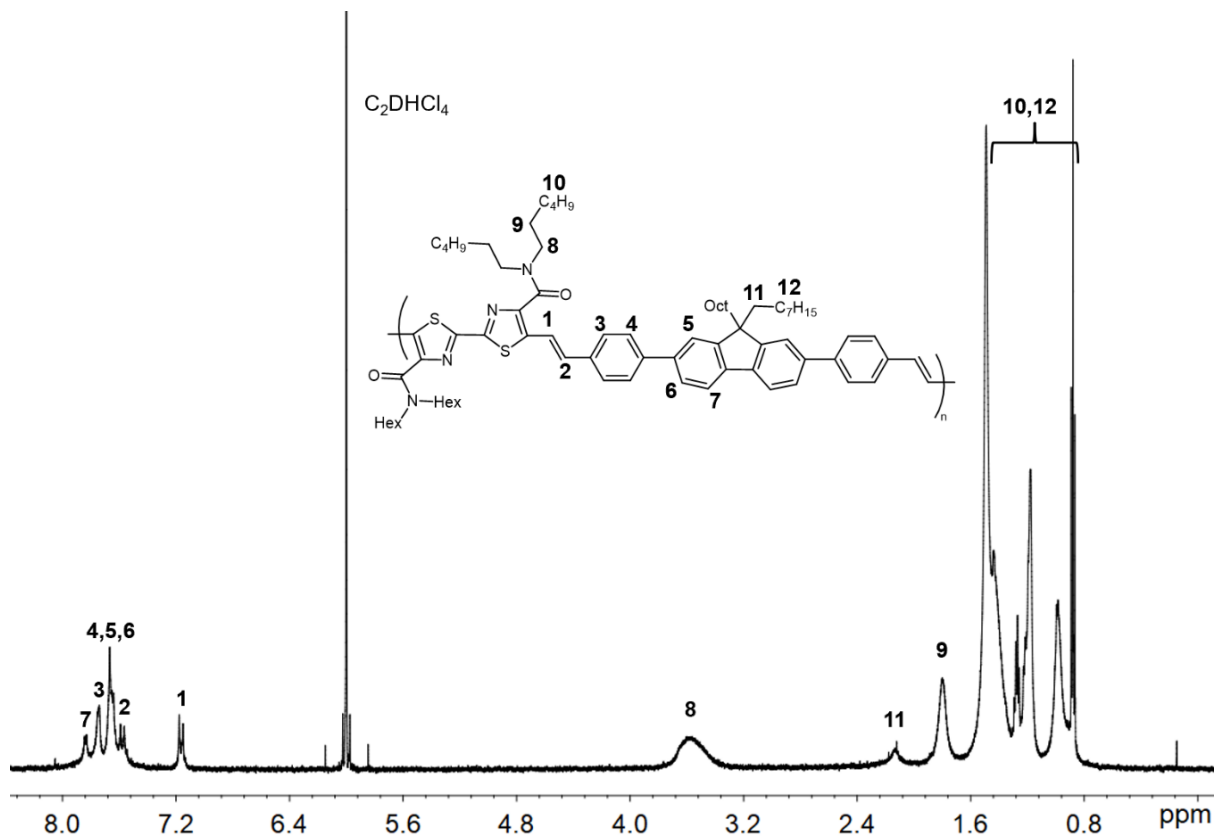


Figure S3.  $^1\text{H}$  NMR spectrum of Pab ( $M_n = 68,000$ , 600 MHz,  $\text{C}_2\text{D}_2\text{Cl}_4$ , 373 K).

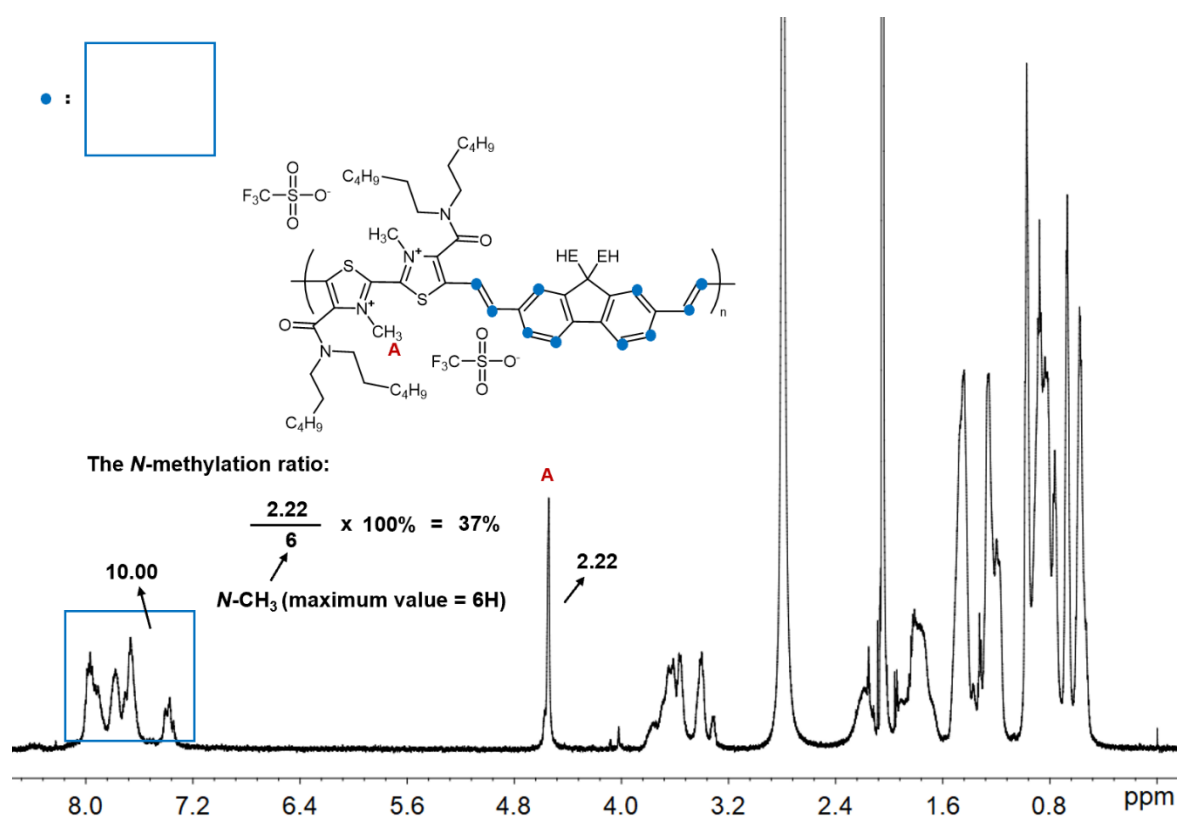


Figure S4. <sup>1</sup>H NMR spectrum of Paa-M-37 (600 MHz, Acetone-*d*<sub>6</sub>, r.t.).

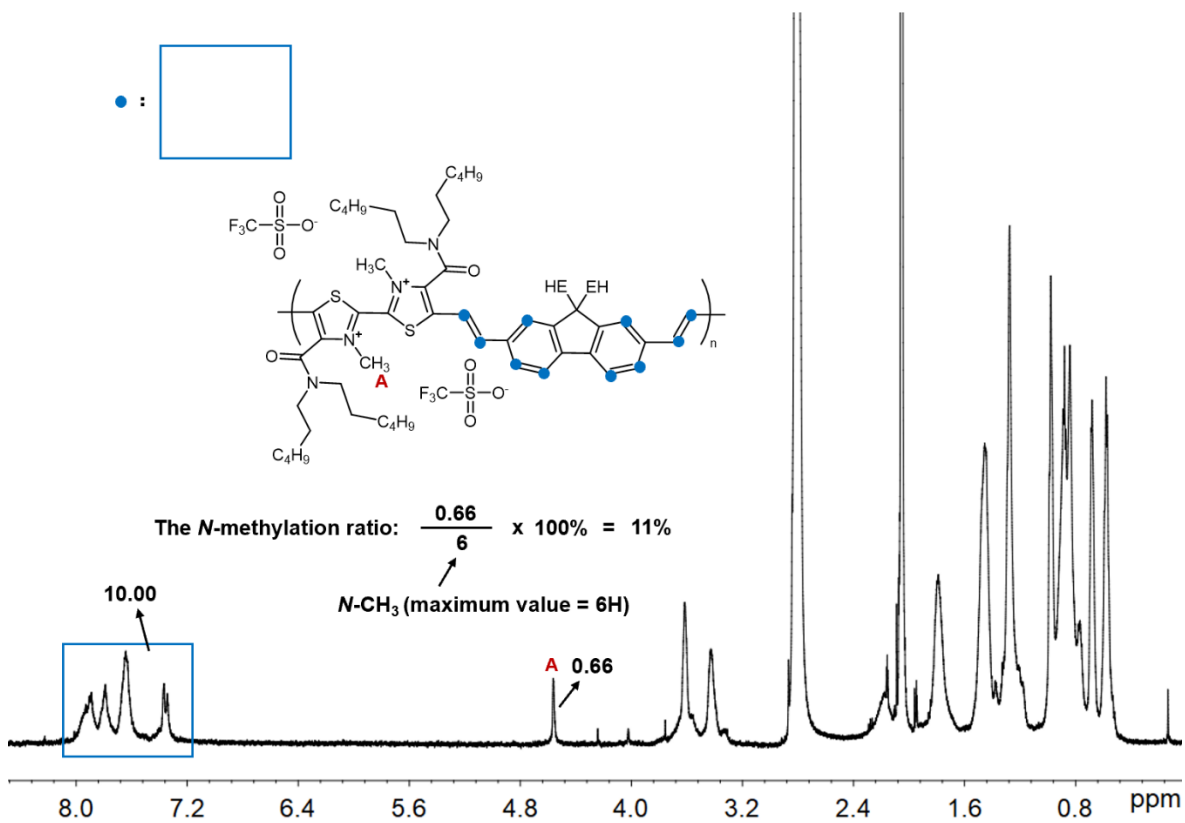


Figure S5. <sup>1</sup>H NMR spectrum of Paa-M-11 (600 MHz, Acetone-*d*<sub>6</sub>, r.t.).

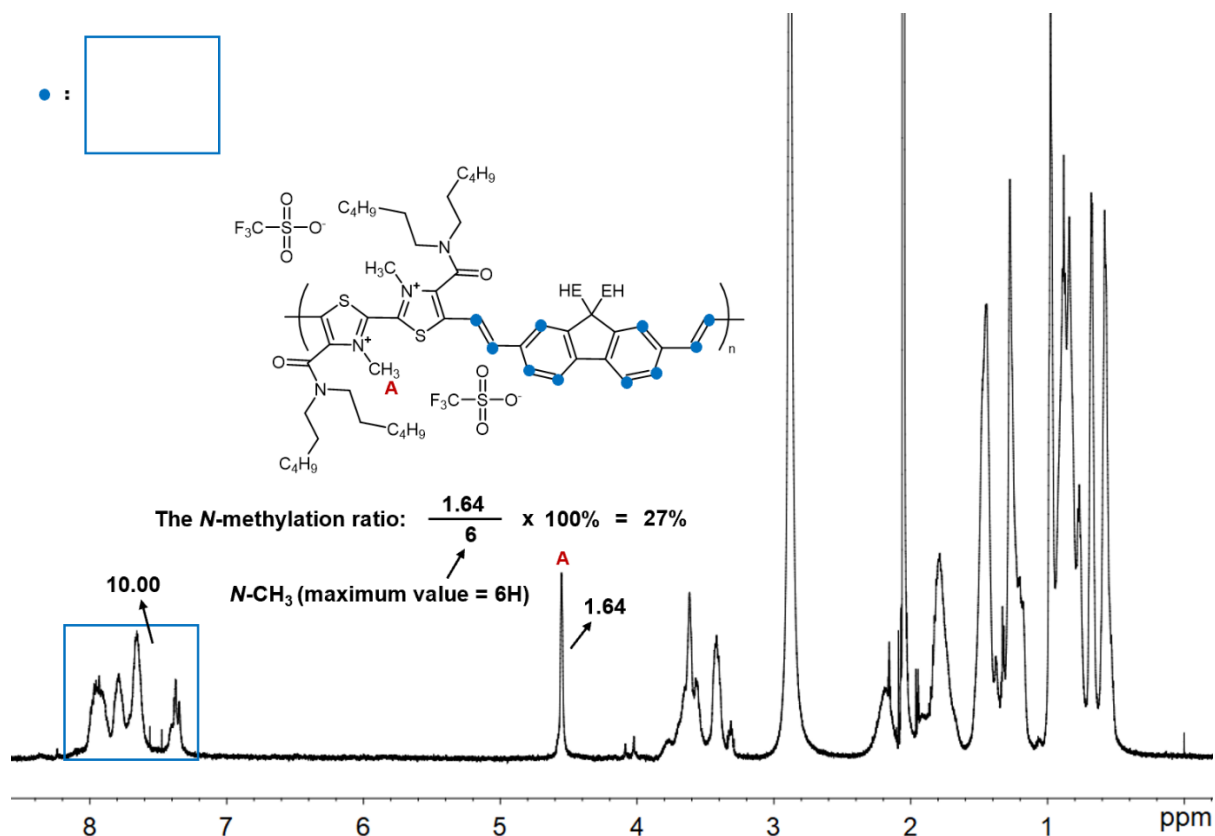


Figure S6. <sup>1</sup>H NMR spectrum of Paa-M-27 (600 MHz, Acetone-*d*<sub>6</sub>, r.t.).

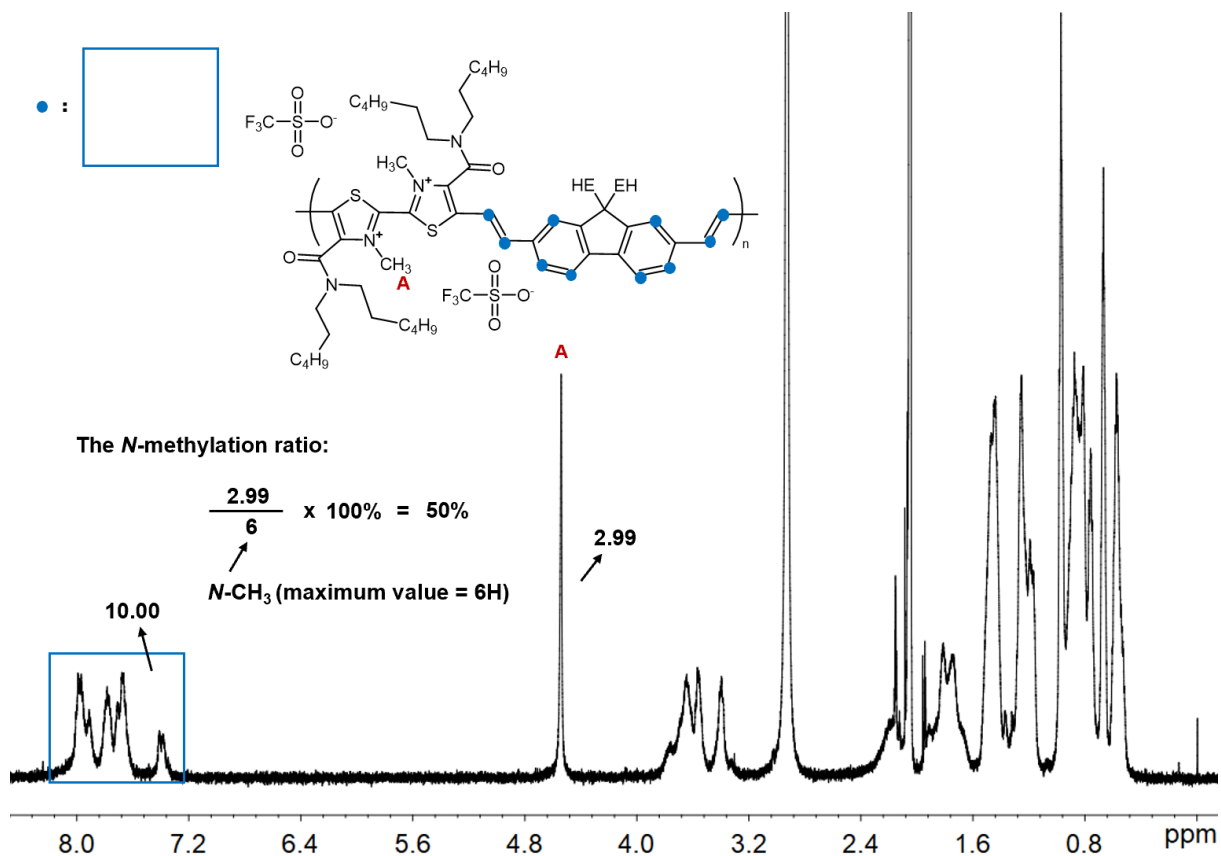


Figure S7. <sup>1</sup>H NMR spectrum of Paa-M-50 (600 MHz, Acetone-*d*<sub>6</sub>, r.t.).

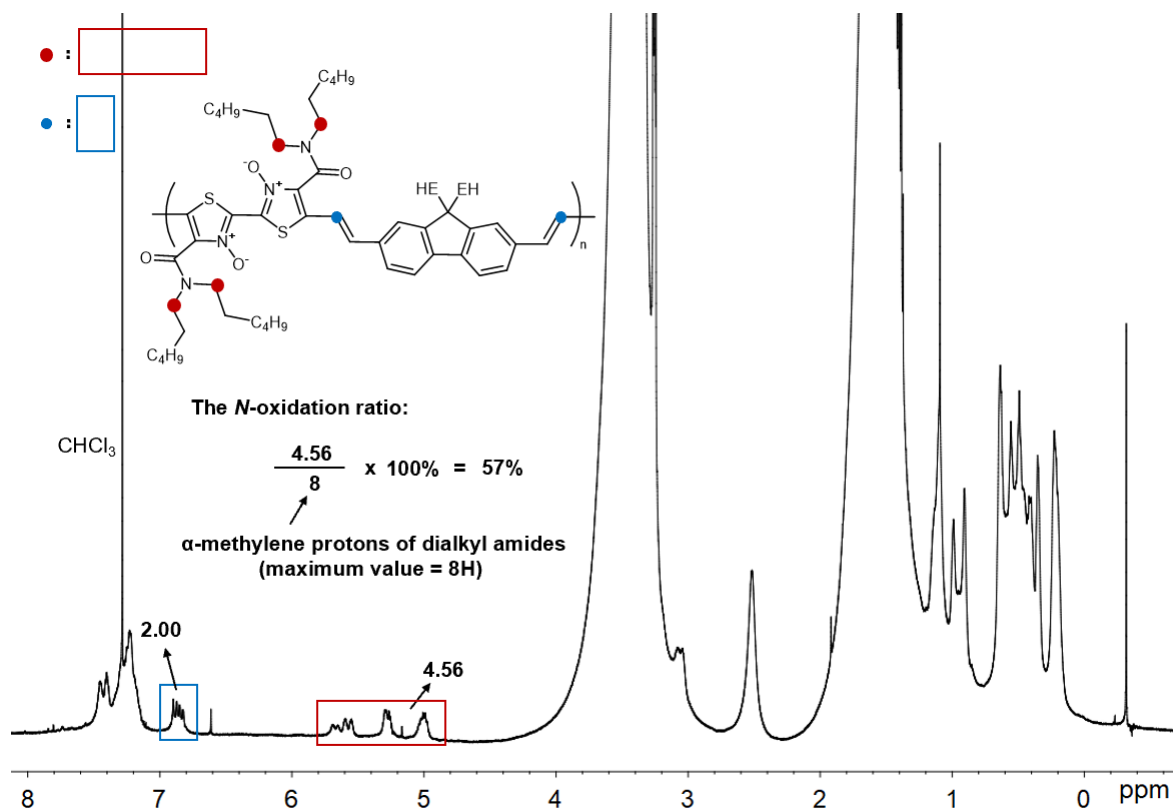


Figure S8. <sup>1</sup>H NMR spectrum of Paa-O (600 MHz, THF/CDCl<sub>3</sub> = 1:1, r.t.).

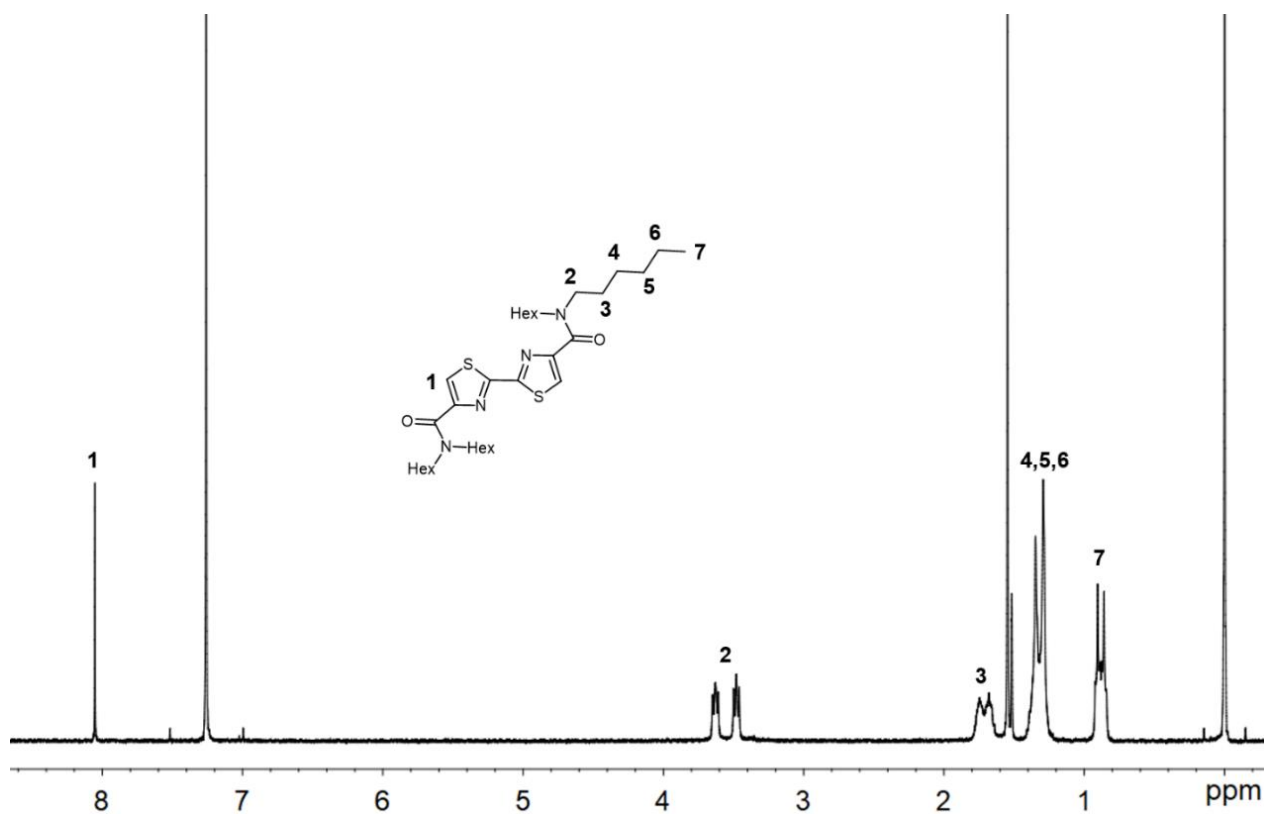
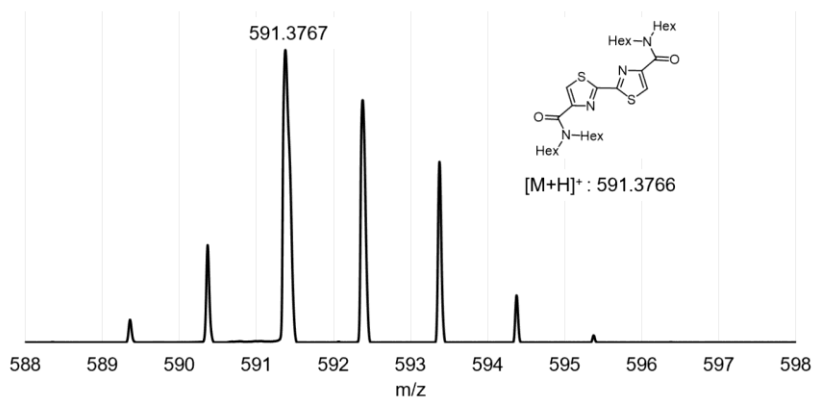
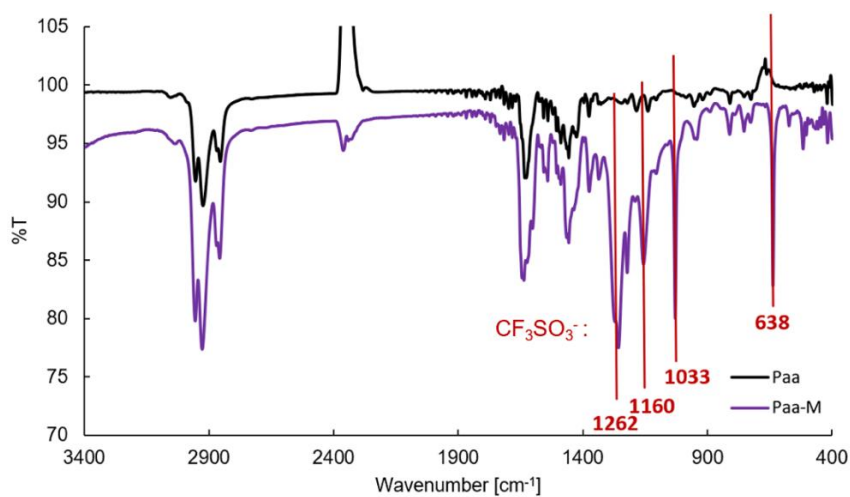


Figure S9. <sup>1</sup>H NMR spectrum of 1a (400 MHz, CDCl<sub>3</sub>, r.t.).



**Figure S10. APCI-MS of 1a.**

**FT-IR spectra**



**Figure S11. FT-IR spectra of Paa and Paa-M.**

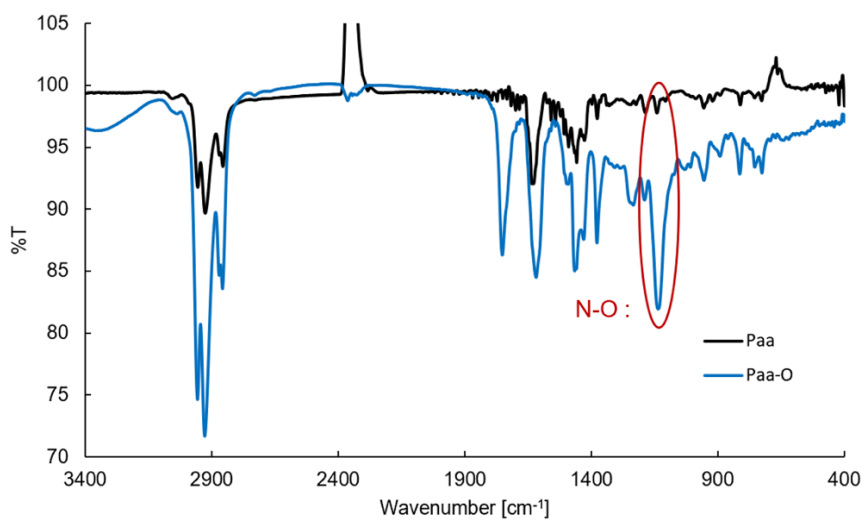


**Figure S12. FT-IR spectra of Paa and Paa-O.**

## GPC charts

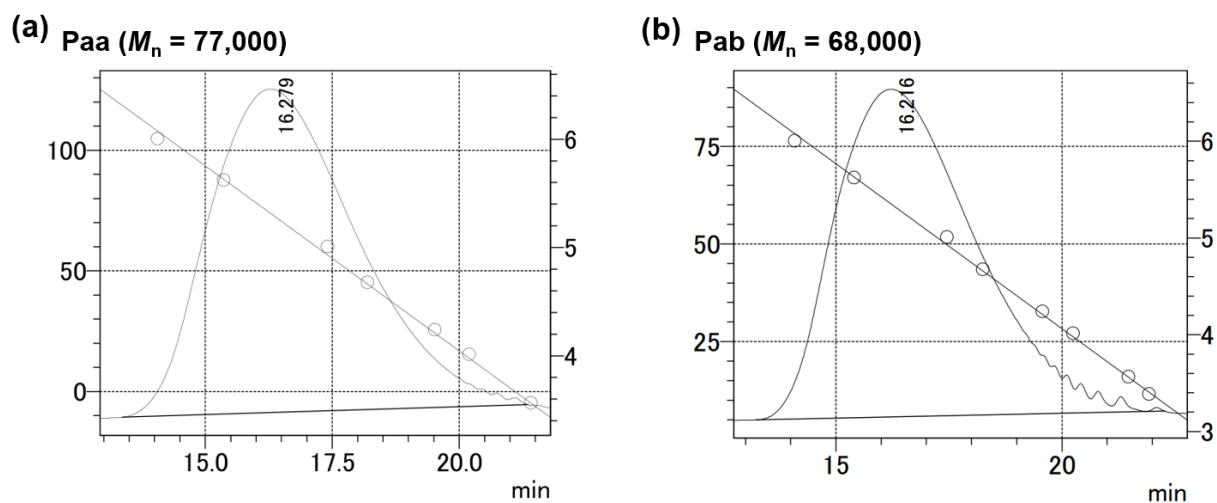


**Figure S13. GPC charts of (a) Paa and (b) Pab (Calibrated on polystyrene standards, Eluent: THF).**

## Optical and electronic data

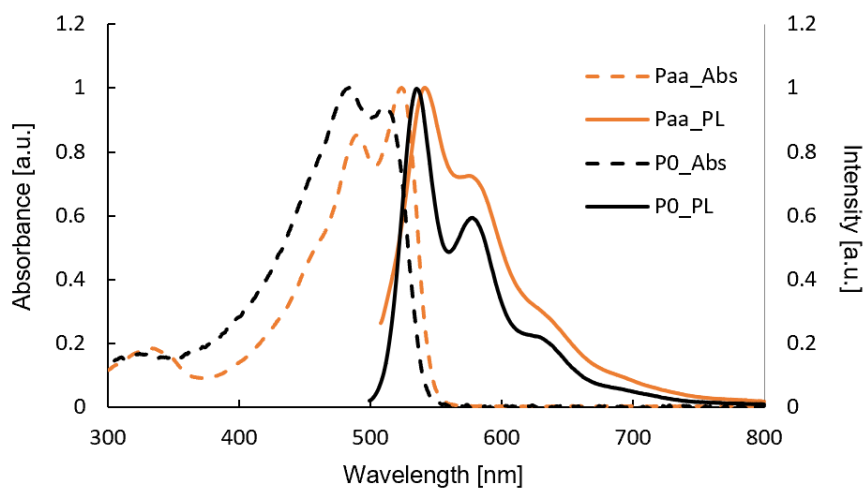
**Table S2. Optical Properties of PAVs in the solution**

PAVs	CHCl <sub>3</sub> solution <sup>a</sup>		
	$\lambda_{\max}$ /nm	$\lambda_{\text{em}}$ /nm	PLQY <sup>b</sup> /%
<b>Paa</b>	524	542	63
<b>P0</b>	484	536	55
<b>Pab</b>	463	557	57
<b>P1</b>	454	513	54
<b>Paa-M-11</b>	520	726	17
<b>Paa-M-27</b>	524	726	20
<b>Paa-M-37</b>	549	725	26
<b>Paa-M-50</b>	577	725	32

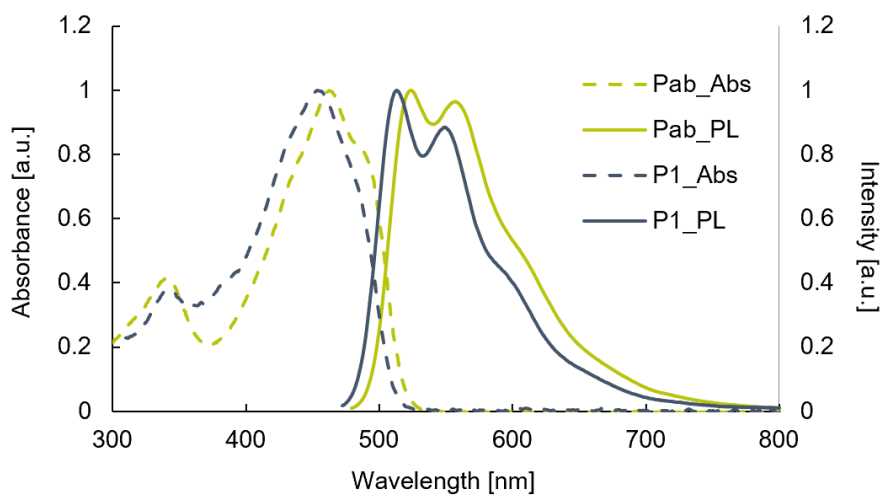
  

PAVs	THF solution <sup>a</sup>		
	$\lambda_{\max}$ /nm	$\lambda_{\text{em}}$ /nm	PLQY <sup>b</sup> /%
<b>Paa</b>	524	542	66
<b>Paa-O</b>	447	537	63

<sup>a</sup> Concentration of  $5.0 \times 10^{-6}$  M. <sup>b</sup> Photoluminescence quantum yield.



**Figure S14. UV-vis absorption and PL spectra of Paa and P0**  
(CHCl<sub>3</sub> solution: 5.0 x 10<sup>-6</sup> M)



**Figure S15. UV-vis absorption and PL spectra of Pab and P1**  
(CHCl<sub>3</sub> solution: 5.0 x 10<sup>-6</sup> M)

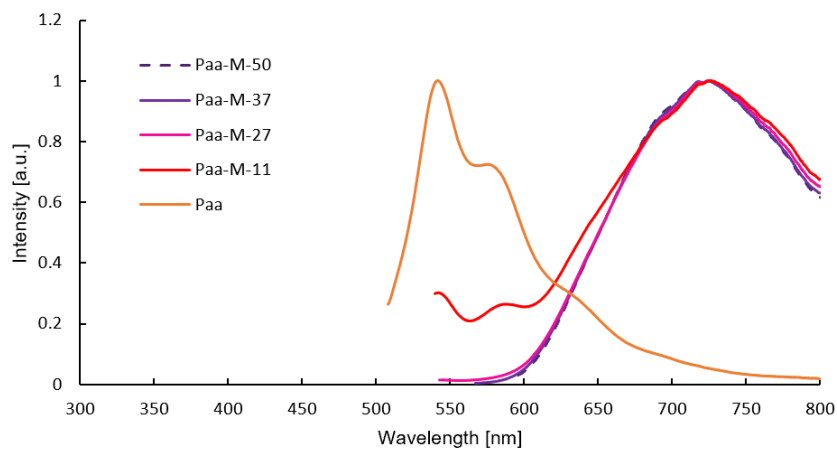


**Figure S16. PL spectra of Paa and Paa-M (CHCl<sub>3</sub> solution: 5.0 x 10<sup>-6</sup> M)**

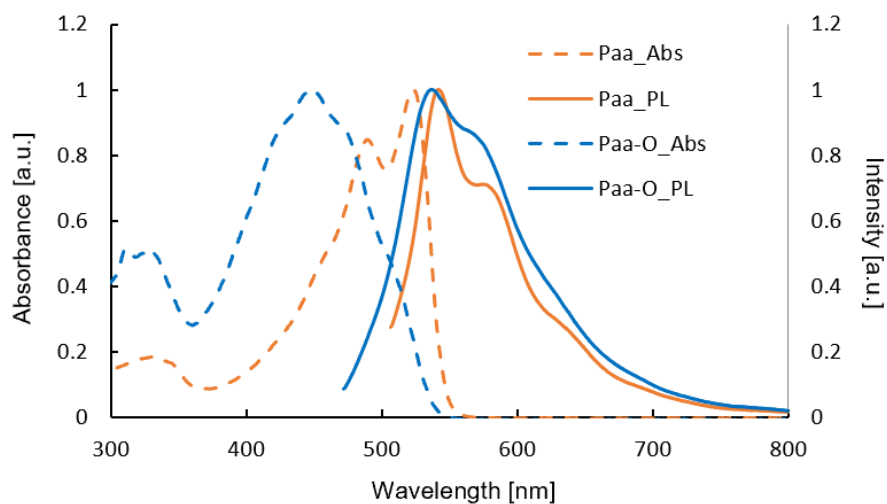


**Figure S17. UV-vis absorption and PL spectra of Paa and Paa-O  
(THF solution:  $5.0 \times 10^{-6}$  M)**

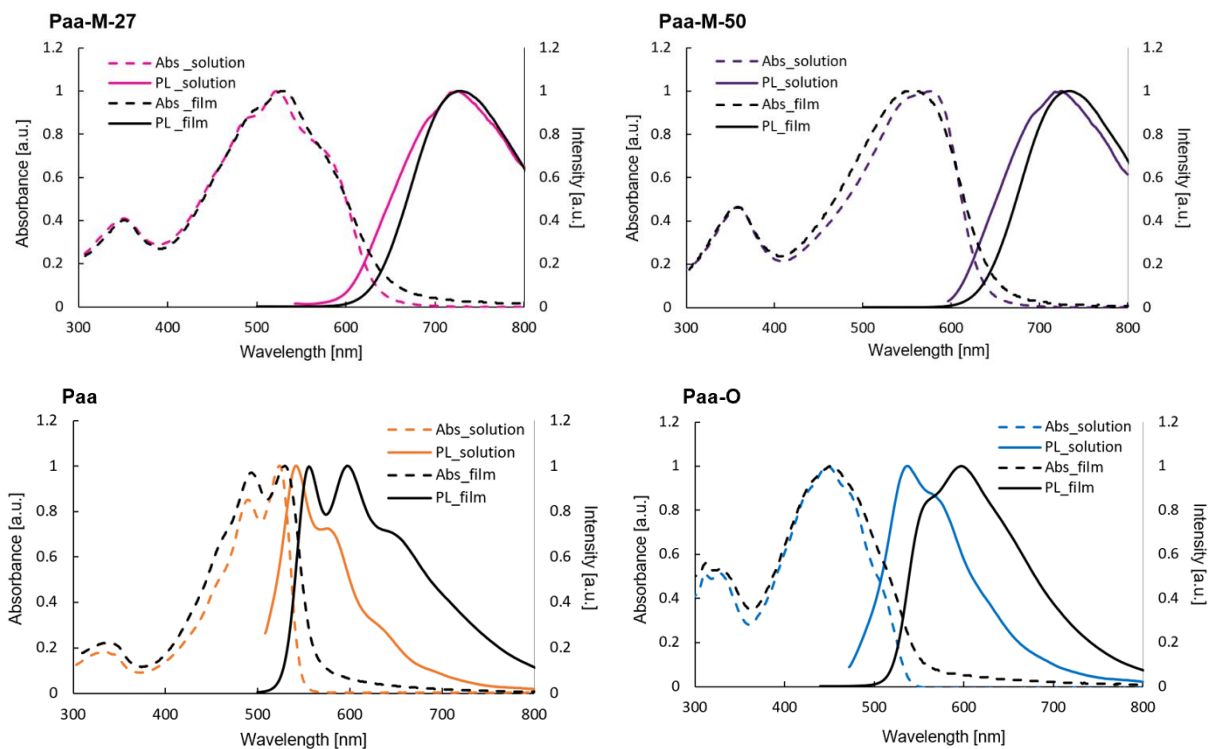


**Figure S18. UV-vis absorption and PL spectra of PAAVs in solution and film states.**

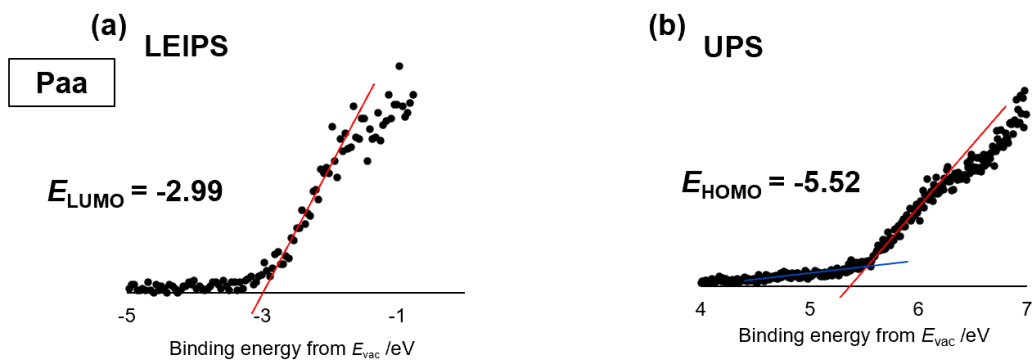


Figure S19. Frontier orbital energy levels analyses of Paa by (a) LEIPS and (b) UPS.

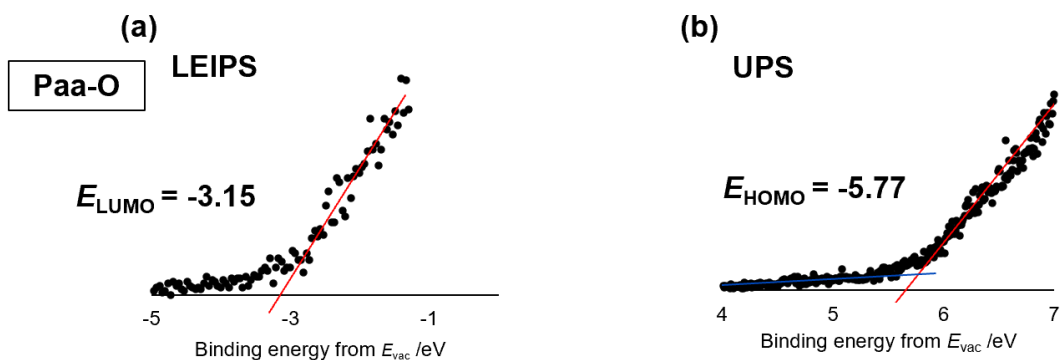


Figure S20. Frontier orbital energy levels analyses of Paa-O by (a) LEIPS and (b) UPS.

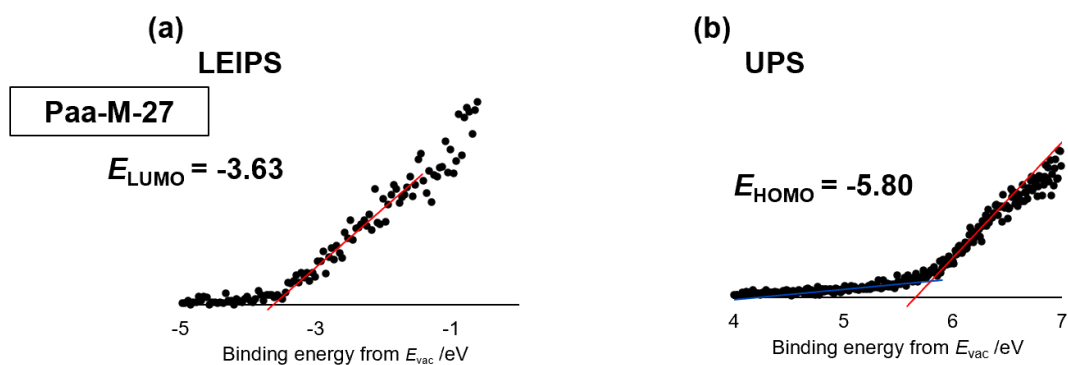
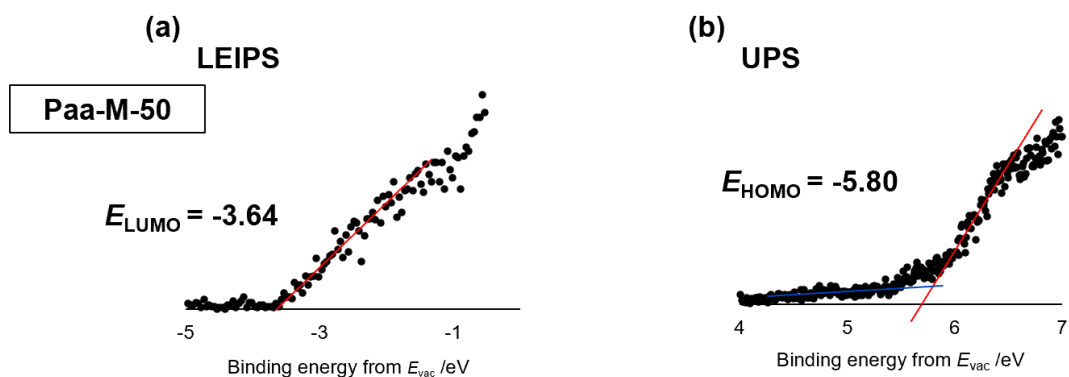
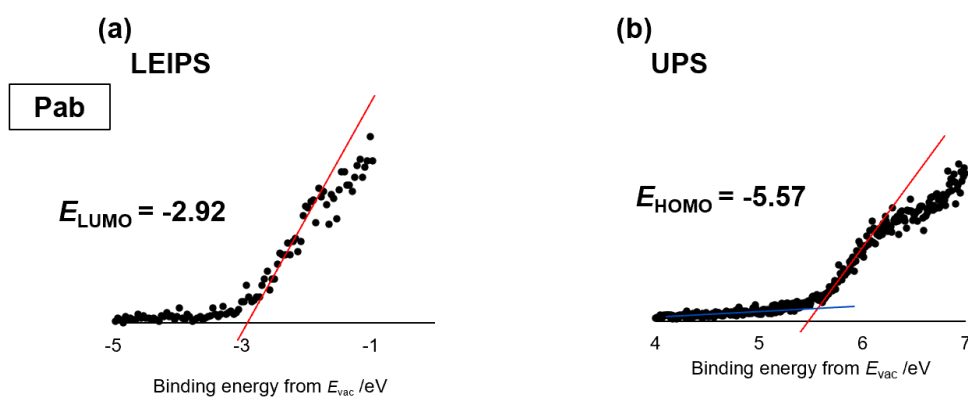


Figure S21. Frontier orbital energy levels analyses of Paa-M-27 by (a) LEIPS and (b) UPS.



**Figure S22. Frontier orbital energy levels analyses of Paa-M-50 by**

**(a) LEIPS and (b) UPS.**



**Figure S23. Frontier orbital energy levels analyses of Pab by (a) LEIPS and (b) UPS.**

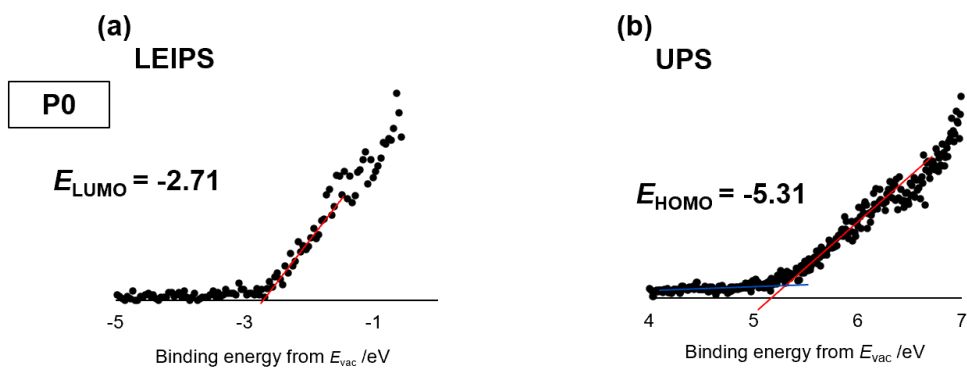


**Figure S24. Frontier orbital energy levels analyses of P0 by (a) LEIPS and (b) UPS.**

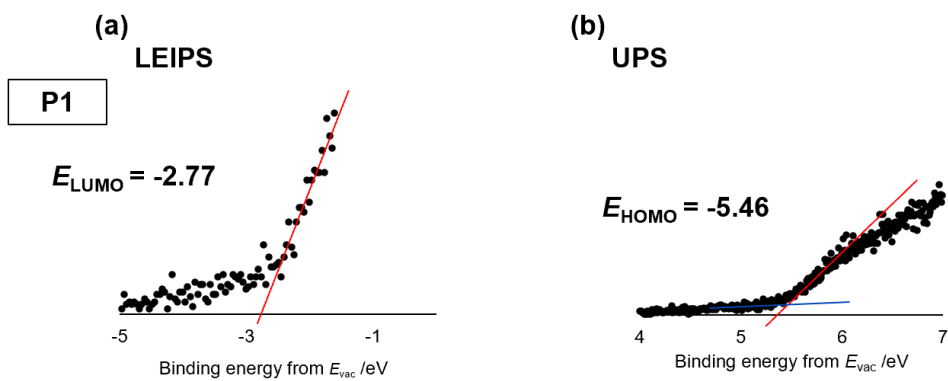


Figure S25. Frontier orbital energy levels analyses of P1 by (a) LEIPS and (b) UPS.

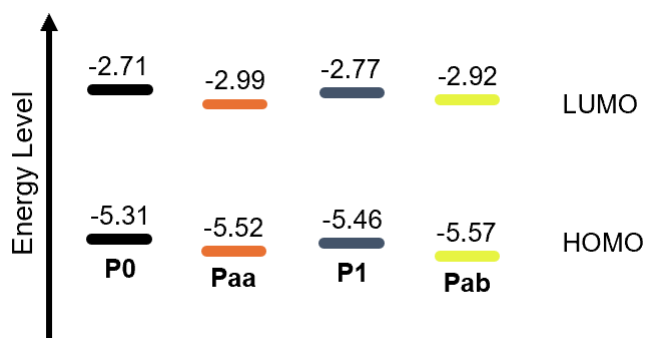


Figure S26. The frontier orbital energy levels of PAVs.

### OLED properties

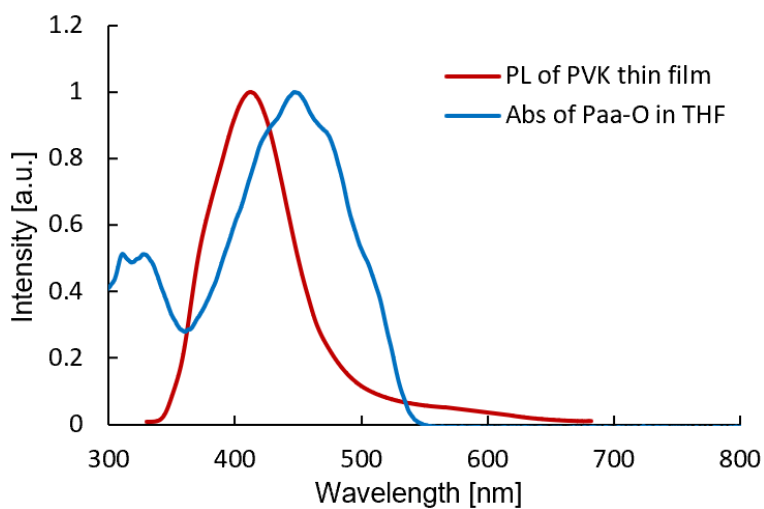
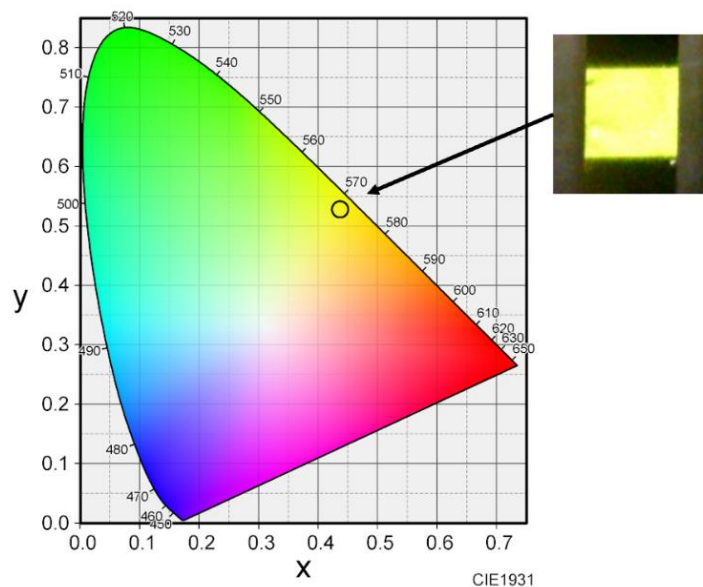
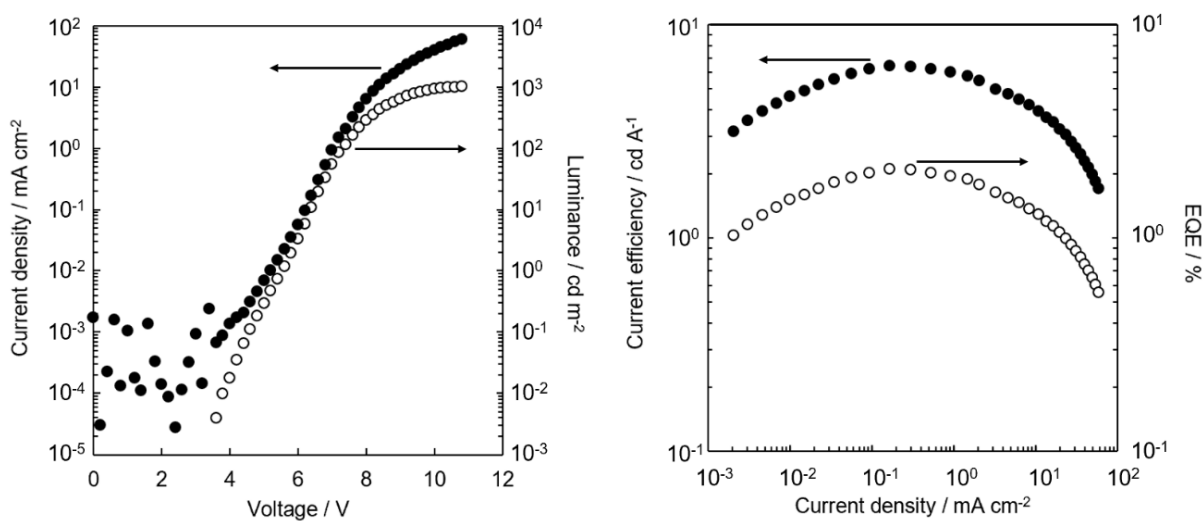


Figure S27. PL of PVK film and Abs of Paa-O in THF ( $5 \times 10^{-6}$  M).



**Figure S28. CIE chromaticity diagram and photo image of OLED using Paa-O.**



**Figure S29. J-V-L curve (left) and current efficiency (EQE) vs. current density plots (right) for OLED using Paa-O.**

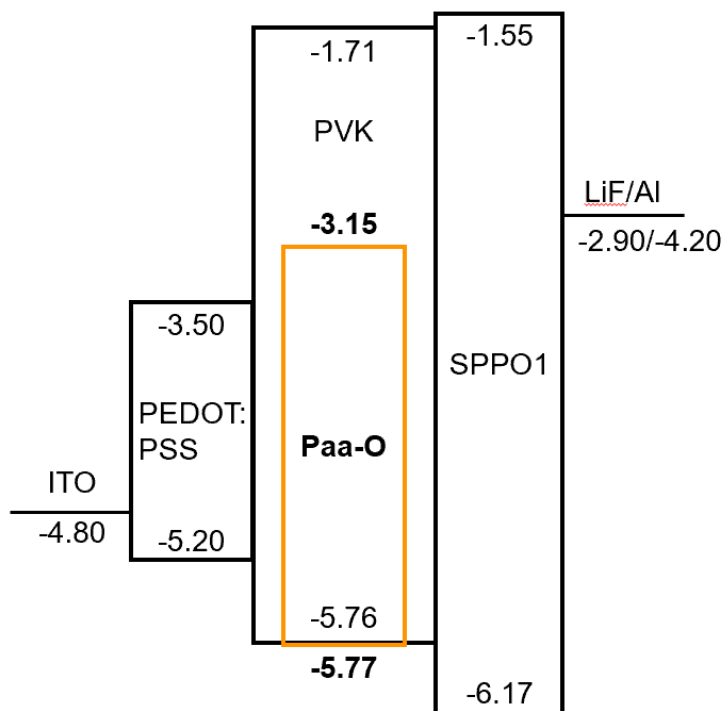


Figure S30. Energy diagram of OLED.

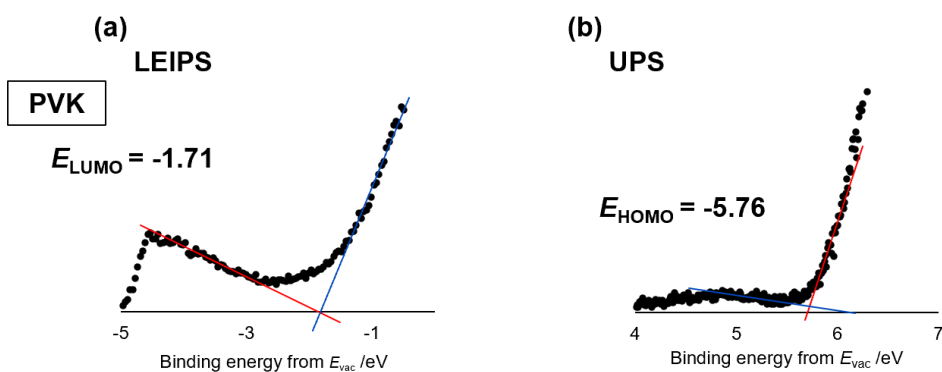


Figure S31. Frontier orbital energy levels analyses of PVK by (a) LEIPS and (b) UPS.<sup>[5,6]</sup>

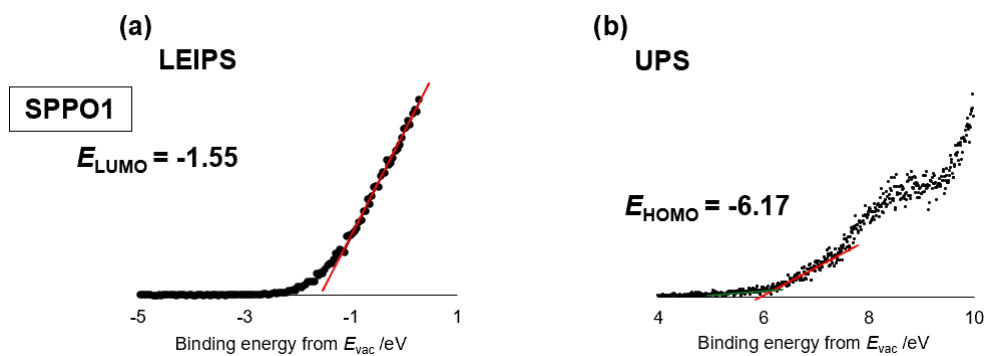


Figure S32. Frontier orbital energy levels analyses of SPPO1 by (a) LEIPS and (b) UPS.

## References

- [1] R. Iwamori, R. Sato, J. Kuwabara, T. Yasuda, T. Kanbara, *Macromol. Rapid Commun.* **2021**, *42*, 202100283.
- [2] X. Zhou, Z. Zhang, A. D. Hendsbee, J. H. L. Ngai, P. Kumar, S. Ye, D. S. Seferos, Y. Li, *RSC. Adv.* **2019**, *9*, 30496-30502.
- [3] T. Yamamoto, A. Morita, Y. Miyazaki, T. Maruyama, H. Wakayama, Z.-H. Zhou, Y. Nakamura, T. Kanbara, S. Sasaki, K. Kubota, *Macromolecules* **1992**, *25*, 1214-1223.
- [4] Y. Shi, W. Li, X. Wang, L. Tu, M. Li, Y. Zhao, Y. Wang, Y. Liu, *Chem. of Mater.* **2022**, *34*, 1403-1413.
- [5] N. A. Talik, B. K. Yap, C. Y. Tan, T. J. Whitcher, *Curr. Appl. Phys.* **2017**, *17*, 1094-1099.
- [6] J. Jeong, J. Lee, H. Lee, G. Hyun, S. Park, Y. Yi, S. W. Cho, H. Lee, *Chem. Phys. Lett.* **2018**, *706*, 317-322.